J Mater Sci (2007) 42:7057–7061
DOI 10.1007/s10853-007-1608-8

Synthesis and characterization of Ti-SBA-16 ordered mesoporous silica composite

Shaodian Shen · Yan Deng · Guibo Zhu · Dongsen Mao · Yuhong Wang · Guishen Wu · Jun Li · XiaoZhen Liu · Guanzhong Lu · Dongyuan Zhao

Received: 19 November 2006 / Accepted: 12 February 2007 / Published online: 5 May 2007

Abstract Ti-SBA-16 mesoporous silica with a cubic *Im3m* structure has been successfully synthesized through prehydrolysis of a silica precursor in the presence of a triblock copolymer F127 under acidic condition. X-ray diffraction (XRD) shows that the highly ordered mesostructure was maintained even at the high loading of titanium up to 5.5 (bulk molar ratio SiO_2/TiO_2). UV–vis and Raman spectroscopy reveal that the titanium species was highly dispersed in the silica framework with tetrahedral coordinate and octahedral coordinate, respectively. N_2-adsorption data exhibit that the BET surface, pore size and pore volume were maintained with an increase of titanium species loading for this cubic *Im3m* mesoporous composite. SEM image shows its amorphous morphology. The synthesis of mesoporous TiO_2-containing SBA-16 composite with a cubic *Im3m* structure will open new applications for catalysts.

Introduction

Mesoporous silica composites containing titanium species have a great deal of application for catalysts due to the titanium's transition metal activity and their large surface area, pore volume and uniform pore size distribution [1–3]. Since the discovery of mesoporous silica M41S [4], various titanium-containing porous silica materials with ordered 2-Dimensional (2-D) or 3-Dimensional (3-D) mesostructure has been synthesized including Ti-MCM-41 [5–8], Ti-MCM-48 [9–12], Ti-SBA-15 [13, 14] and Ti-SBA-1 [15]. Recent progress mainly focuses on the synthesis of Ti-containing mesoporous silica composite with different structure, due to the fact that the different mesostructure in the Ti-containing composite possess different pore channel connectivity, which will allow different molecules come into and out of the pore system. As compared with 2-D hexagonal mesoporous Ti-containing composite, a cubic mesoporous TiO_2/Silica composites is probably more favorable to be applied to catalysts than 2-D hexagonal structure, because its 3-D connectivity will allow large molecules diffuse easily.

Ti-containing mesoporous silica can be fabricated by directly incorporating the titanium species into the silica framework through a hydrolysis-condensation process, and $TiCl_4$ and TEOS are generally used as precursors. However, the hydrolysis rate for $TiCl_4$ is faster than that for TEOS, and thus will lead to the non-homogenously deposition of titanium species onto the mesoporous silica walls when the silica precursor was added together with $TiCl_4$, and titania-silica mixture with collapsed mesostructure was obtained. To avoid this phenomenon, it is necessary to select a suitable titanium or silicon precursor to control their different hydrolysis rate so as to fabricate a well-ordered Ti-containing mesoporous silica composite. Li and co-workers [8] select an inorganic $TiCl_3$ solution with relatively low hydrolysis instead of a $TiCl_4$ precursor to synthesis Ti-MCM-41 mesoporous composite, and isolated Ti^{4+} ions were found, which means titanium species were highly dispersed on the silica framework. Accelerating the silicon precursor's hydrolysis rate using fluoride catalysis

S. Shen (✉) · D. Mao · Y. Wang · G. Wu · J. Li · XiaoZhen Liu · G. Lu
Department of Chemical Engineering, Shanghai Institute of Technology, Shanghai 200235, China
e-mail: shaodian85@yahoo.com.cn

S. Shen · Y. Deng · G. Zhu
Unilever Research China, Shanghai, China

D. Zhao
Department of Chemistry, Fudan University, Shanghai 200433, China

is another selectable method to manufacture the Ti-SBA-15 mesoporous silica [14], while the low titanium content in this composite restrict their further application to catalysts.

Since the hydrolysis rate of silicon precursor is slower than that of $TiCl_4$, through prehydrolysis [16–18] of the silica precursor such as TEOS followed by adding titanium precursor is another ideal method for the synthesis of a Ti-containing silica composite. This method can facilitate the titanium species to be incorporated effectively into the silica framework and lead to the synthesis of TiO_2/SiO_2 mesoporous composite with high titania content, which will have the high catalysis reactivity during the catalysis process.

SBA-16 is a newly discovered mesoporous silica molecular sieve with large cage *Im3m* structure [19, 20]. It possesses high hydrothermal stability due to its thick pore wall and 3-D cage structure that have a promising application to catalysts and catalytic carriers. To the best of our knowledge, the synthesis of a well ordered Ti-SBA-16 composite with a high amount of Titanium species on silica framework under the method of prehydrolysis of precursor and its characterization have not been clearly reported in the open literature so far.

In this present study, a cubic *Im3m* Ti-SBA-16 mesoporous silica composite with different titania concentration have been prepared through prehydrolysis of TEOS followed by adding the $TiCl_4$ process. The synthesized TiO_2/Silica mesoporous composite possess highly ordered cubic *Im3m* structure, in addition, high TiO_2 content in this composite (loading up to SiO_2/TiO_2 molar ratio of 5.5) can be dispersed in the silica surface and wall. A systematic investigation of Ti-SBA-16 materials by powder X-ray diffraction (XRD), nitrogen adsorption/desorption, diffuse reflectance UV–visible (UV–vis), Laser Raman spectroscopy and Scanning electron micrographs (SEM) were carried out for their characterization.

Experimental section

Ti-containing SBA-16 composites with different concentrations of titanium have been prepared under an acidic condition in the presence of tri-block copolymer F127 by using tetraethyl orthosilicate (TEOS) as silica source and $TiCl_4$ as Ti source. Typical synthesis of TiO_2/Silica composite is as follows: 1.6 g of F127 was dissolved in the 40 g of 2.0 M HCl under magnetic stirring to obtain a homogeneous solution at 30 °C, to this solution was added 3.4 g of TEOS. After the mixed solution was further vigorously stirred for 30 min to prehydrolysize the TEOS, a pre-requisite amount of $TiCl_4$ was added to give a bulk Si/Ti molar ratio of ∞ (pure silica), 11, 5.5, and 2.7, respectively. The mixture solution was further stirred for another 24 h and then placed in a Teflon bottle and heated to 80 °C for 1 day. The as-synthesized TiO_2/SiO_2 mesoporous composite was filtered, and dried in the air. Template free products were obtained by calcination the as-synthesized sample in air at 550 °C for 6 h.

Characterization

Powder XRD patterns were recorded with Bruker D4 Powder X-ray diffractometer using Cu Kα radiation. Nitrogen adsorption measurements were carried out on a Tristar 3000 volumetric adsorption analyzer. Before the adsorption measurements, the samples were outgassed at 200 °C in the port of the adsorption analyzer. The UV–visible spectra were measured with a Cary 5 UV–vis–NIR spectrophotometer equipped with the Varian diffuse reflectance attachment.

Raman spectra were measured with Dilor LabRam-1B micro-Raman spectrum, using an excitation laser at 633 nm. The spectra were recorded at room temperature by the condition of 50 s integral time at a 1 cm^{-1} resolution. Scanning electron micrographs (SEM) were taken on a XL 30 Philips 20 kV.

Results and discussion

X-ray diffraction analysis

As shown in Fig. 1a, calcined pure silica SBA-16 templated with tri-block polymer F127 exhibited a well-resolved XRD pattern with a sharp diffraction peak and two weak diffraction peaks corresponding to d-spacing of 12.78, 9.00, and 7.26 nm, respectively. These three diffraction peaks can further been indexed as 110, 200, 211, which is a typical characteristic pattern with cubic *Im3m* mesostructure with a cell parameter a = 18.07 nm that matched well with the pattern reported [19, 20].

Calcined mesoporous Ti-SBA-16 gave a fairly well-ordered cubic structure with bulk Si/Ti molar ratio larger than 5.5 (Fig. 1c), and element analysis showed the Si/Ti molar ratio in the final product to be 86.4:1, suggesting the current approach for prehydrolysis of precursor TEOS is an effective method to synthesize the TiO_2/Silica cubic *Im3m* mesoporous composite with high titania content. The mesostructure collapsed with the increase of titanium content up to SiO_2/TiO_2 bulk molar ratio of 2.7 (see Fig. 1d).

UV–visible spectroscopy

UV–visible spectroscopy is an effective technique for revealing the state of titanium species in the porous silica composite**.** The UV–vis spectra for Ti-SBA-16 mesoporous

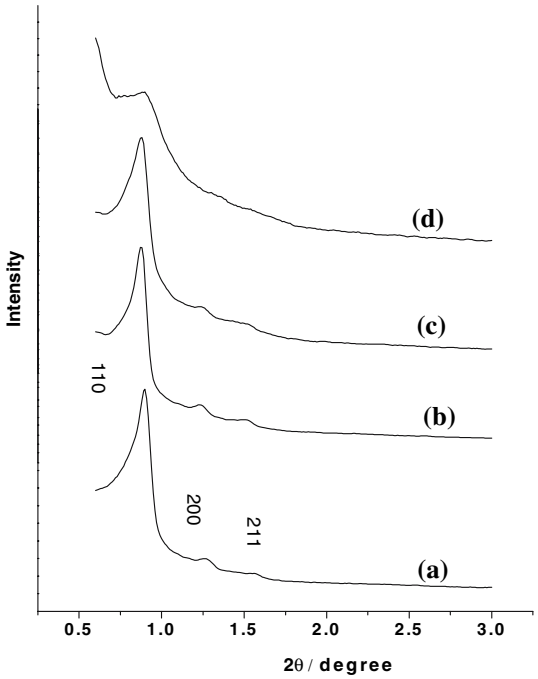

Fig. 1 XRD patterns for pure cubic *Im3m* SBA-16 and its Ti-substitute mesoporous silica composites with different Titania content (SiO_2/TiO_2): (**a**) ∞ (SBA-16); (**b**) 11; (**c**) 5.5; and (**d**) 2.7

silicas, and pure TiO_2 (anatase) are shown in Fig. 2. Pure anatase TiO_2 (Fig. 2d) exhibits broad absorption peak at UV region from 200 to 380 nm. Well-ordered Ti-SBA-16 product (Fig. 2a, b) exhibit two main absorptions at 210 and 235 nm, which can be assigned to isolated tetrahedral (Td) and octahedral (Oh) titanium species, respectively, suggesting all these titanium species are present within the walls or near the surface for mesoporous SBA-16. A broad absorption peak at about 320 nm can be further observed for the high-loading titania composites (Fig. 2c) and can be regarded as the result of some Ti–O–Ti linkages formed during calcination as part of small TiO_2 regions [9].

Raman spectroscopy

Raman spectroscopy technique is a perfect approach to characterize the bulk titania within or on the surface of the mesoporous silica since it is very sensitive to the polarize Ti–O bond features mainly absorbing at 144 cm^{-1} for the anatase phase (Fig. 3d) [9, 10]. As shown in Fig. 3a, no sign of the most intense absorbance at 144 cm^{-1} can be observed for the mesoporous silica composite with low-loading of Titanium, indicating there was not bulk crystalline titania in the cubic Ti-SBA-16 mesoporous silica composites and Titania was highly dispersed in the wall and the surface of these samples. While at relatively high content of titanium in cubic *Im3m* Ti-SBA-16 composite (Fig. 3b), slight absorbance signal was received at 144 cm^{-1}, suggesting the bulk titania (anatase phase) begin

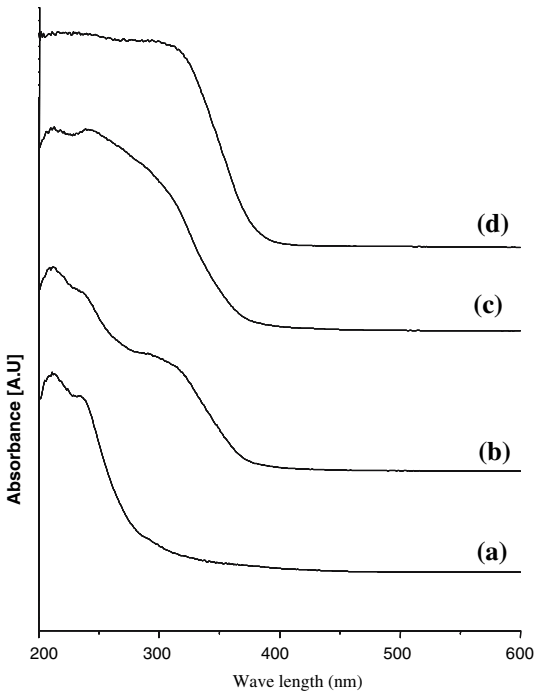

Fig. 2 UV–visible spectra of Ti-SBA-16 with SiO_2/TiO_2 of (**a**) 11; (**b**) 5.5; (**c**) Ti-SBA-16 with collapsed structure with Ti content of 2.7 and (**d**) pure TiO_2

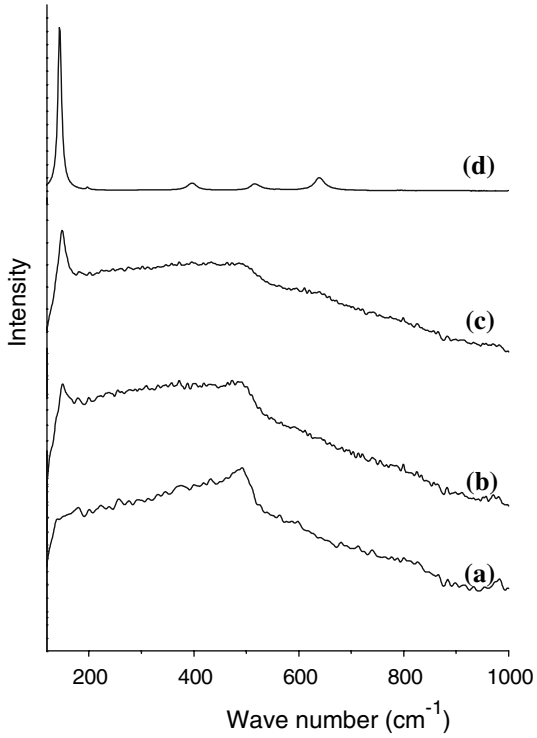

Fig. 3 Raman spectra of calcined Ti-SBA-16 composite at SiO_2/TiO_2 molar ratio with (**a**) 11; (**b**) 5.5; (**c**) 2.7 and (**d**) pure TiO_2 with anatase phase

to be formed. Furthermore, more intense absorbance at 144 cm^{-1} can be observed in Raman spectra for Ti-composite with collapsed mesostructure (Fig. 3c), revealing there was large amount of bulk anatase titania domain in the Ti-containing composite. The phenomena also confirmed the cause why increase the concentration of titanium will lead to the collapse of cubic mesostructure.

N_2 adsorption–desorption measurement

Ti-SBA-16 mesoporous silica composites exhibit relatively large BET surface area, and high pore volume as well as large pore size (Table 1). For the Ti-containing silica composite with a SiO_2/TiO_2 ratio of 11, the BET surface area is as large as 481 m^2/g and BJH pore volume is 0.114 cm^3/g. N_2-sorption data gives IV type curves for SBA-16 and Ti-SBA-16 composites with different titanium content (Fig. 4). A relatively large hysteresis loop can be observed at P/P_o 0.4–0.6 in the pure SBA-16 silica (Fig. 4a), and the cubic cage mesostructure maintained when the titanium dioxide content is relatively low (Fig. 4c). The hysteresis loop decreases gradually upon further increasing the titanium content, indicting its mesostructure was collapsed in the high Ti-content composite (Fig. 4d).

Table 1 Physical properties for Ti-SBA-16 mesoporous silica composite

Sample	SiO_2/TiO_2 molar ratio	S_{BET} (m^2 g^{-1})	Pore volume BJH (cm^3 g^{-1})	Pore diameter BJH[a] (nm)
SBA-16		492	0.131	3.8
Ti-SBA-16	11	481	0.114	3.33
Ti-SBA-16	5.5	486	0.113	3.41
Ti-SBA-16	2.7	465	0.105	3.60

[a] The pore diameter calculated using the BJH method for cylindrical pores (the actual diameter of spherical pores of SBA-16 is likely higher than the values provided)

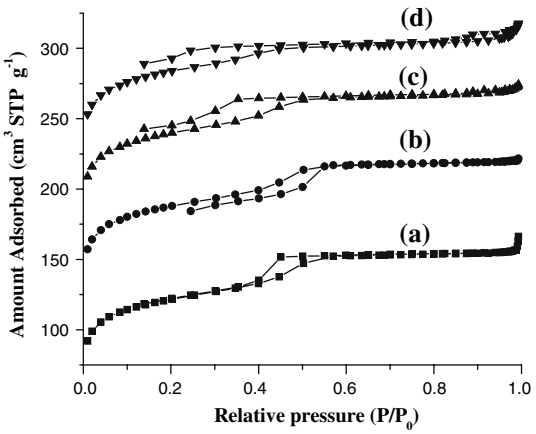

Fig. 4 N_2-sorption isotherms for calcined Ti-SBA-16 composite with different Titania loadings (Si/Ti molar ratio): (**a**) ∞; (**b**) 11; (**c**) 5.5; and (**d**) 2.7. The isotherms for **b**, **c** and **d** are offset vertically by 50, 100 and 150 cm^3 STP g^{-1}, respectively

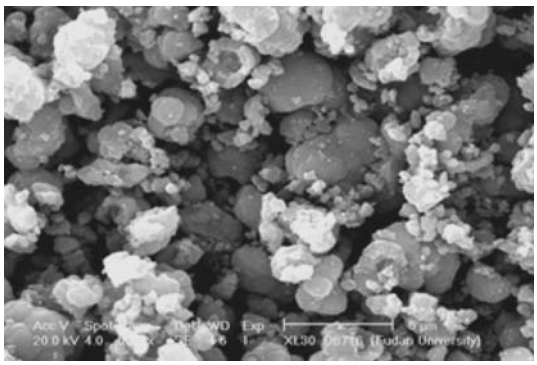

Fig. 5 SEM image for Ti-SBA-16 mesoporous silica with a SiO_2/TiO_2 molar ratio of 5.5

Scanning electron micrograph (SEM) observation

SEM image (Fig. 5) shows that Ti-SBA-16 mesoporous sililca composites have non-uniform particle morphology with the size of about 1–2 mm, which is similar to that for SBA-16 prepared under acidic conditions.

Conclusion

Highly ordered mesoporous TiO_2/Silica composites with cubic *Im3m* structure have been successfully prepared through a simple, two-step prehydrolysis method using TEOS and $TiCl_4$ as Silica and Ti resource, respectively. X-ray diffraction, UV–vis and laser Raman spectrum characterized their high ordered mesostructure and were maintained even when a relatively high titanium species concentration was loaded. N_2 sorption exhibits their high surface area, large pore volume and high pore size. The synthesized TiO_2 hybrid composites with high titania content provide the potential possibility of high efficiency for catalysis in the fine chemistry and other photo catalysts.

Acknowledgements Shaodian SHEN thanks Shanghai Institute Technology for leading academic discipline project (P1501).

References

1. Corma A (1997) Chem Rev 97:2373
2. Kholdeeva OA, Trukhan NN (2006) Russ Chem Rev 75(5):411
3. Orlov A, Zhai Q-Z, Klinowski J (2006) J Mater Sci 41:2187

4. Kresge CT, Leonowica ME, Rogh WJ, Vartuli JC, Beck JS (1992) Nature 359:710
5. Maschmeyer T, Rey F, Sankar G, Thomas JM (1995) Nature 378:159
6. Corma A, Navarro MT, Perrez-Pariente JJ (1994) Chem Soc Chem Commun 147
7. Anpo M, Yamashita H, Ikeue K, Fujii Y, Zhang SG, Ichihashi Y, Park DR, Suzuki Y, Koyano K, Tatsumi T (1998) Catal Today 44:327
8. Yu J, Feng Z, Xu L, Li M, Xin Q, Liu Z, Li C (2001) Chem Mater 13(3):994
9. Morey MS, Brien SO, Schwarz S, Stucky GD (2000) Chem Mater 12(4):898
10. Morey MS, Davidson A, Stucky GD (1998) J Porous Mater l5(3–4):195
11. Morey MS, Davidson A, Stucky GD (1996) Micro Mater 6(2):99
12. Koyano KA, Tatsumi T (1996) Chem Commun 2:45
13. Luan ZH, Estelle MM, Van Der Heide PAW, Zhao DY, Czernuszewica RS, Kevan L (1999) Chem Mater 11:3680
14. Zhang W-H, Lu J, Han B, Li M, Xiu J, Ying P, Li C (2002) Chem Mater 14(8):3413
15. Ji D, Zhao R, Lv G, Qian G, Yan L, Suo J (2005) Appl Catal A Gen 281(1–2):39
16. Scharml-Marth M, Walther KL, Wokan A, Handy BE, Baiker A (1992) J Non-Cryst Solids 143:93
17. Delange RSA, Hehhink JHA, Keelzer K, Burggraaf AJ (1995) J Non-Cryst Solids 191:1
18. Pereira MM, Clarck AE, Hench LL (1994) J Mater Synth Process 2:3
19. Zhao D, Huo Q, Feng J, Chmelka BF, Stucky GD (1998) J Am Chem Soc 120(24):6024
20. Zhao D, Feng J, Huo Q, Melosh N, Fredrickson GH, Chemlka BF, Stucky GD (1998) Science 279:548